Biochemical and Crystallographic Characterization of Ferredoxin−$NADP^+$ Reductase from Nonphotosynthetic Tissues[†,‡]

Alessandro Aliverti,[§] Rick Faber,[∥] Casey M. Finnerty,[⊥] Cristian Ferioli,[§] Vittorio Pandini,[§] Armando Negri,[@] P. Andrew Karplus,[∥] and Giuliana Zanetti*[,§]

Dipartimento di Fisiologia e Biochimica Generali, Università degli Studi di Milano, Via Celoria 26, 20133 Milano, Italy, Department of Biochemistry and Biophysics, Oregon State University, Corvallis, Oregon 97331, Department of Molecular Biology and Genetics, Cornell University, Ithaca, New York 14853, and Istituto di Fisiologia Veterinaria e Biochimica, Via Celoria 10, 20133 Milano, Italy

Received June 13, 2001; Revised Manuscript Received September 19, 2001

ABSTRACT: Distinct forms of ferredoxin−$NADP^+$ reductase are expressed in photosynthetic and nonphotosynthetic plant tissues. Both enzymes catalyze electron transfer between NADP(H) and ferredoxin; whereas in leaves the enzyme transfers reducing equivalents from photoreduced ferredoxin to $NADP^+$ in photosynthesis, in roots it has the opposite physiological role, reducing ferredoxin at the expense of NADPH mainly for use in nitrate assimilation. Here, structural and kinetic properties of a nonphotosynthetic isoform were analyzed to define characteristics that may be related to tissue-specific function. Compared with spinach leaf ferredoxin−$NADP^+$ reductase, the recombinant corn root isoform showed a slightly altered absorption spectrum, a higher pI, a >30-fold higher affinity for $NADP^+$, greater susceptibility to limited proteolysis, and an ∼20 mV more positive redox potential. The 1.7 Å resolution crystal structure is very similar to the structures of ferredoxin−$NADP^+$ reductases from photosynthetic tissues. Four distinct structural features of this root ferredoxin−$NADP^+$ reductases are an alternate conformation of the bound FAD molecule, an alternate path for the amino-terminal extension, a disulfide bond in the FAD-binding domain, and changes in the surface that binds ferredoxin.

In 1990, it became established that a distinct isoform of ferredoxin−$NADP^+$ reductase (FNR,[1] EC 1.18.1.2), the flavoprotein responsible for the production of NADPH during photosynthesis, was present in plastids of nonphotosynthetic tissues (*1*−*3*). The root isoform of FNR was postulated to work in the opposite direction compared to chloroplast FNR, providing reduced Fd for Fd-dependent enzymes present in the roots. Involvement in nitrogen assimilation was inferred from the observations that a protein immunoreactive with antibodies against leaf FNR was induced in pea roots exposed to nitrate (*4*), and cDNAs encoding a root FNR were isolated from libraries constructed from the roots of nitrate-induced rice and maize seedlings (*5*, *6*). This regulation of expression contrasts with that of chloroplast FNR, which is under the control of light (*7*).

The sequences of the isoforms of roots and leaves from the same species (rice or corn) are ∼48% identical, whereas leaf FNRs from different higher plants are more than 80% identical. Construction of a phylogenetic tree with 13 known FNR sequences (*8*) revealed that the nonphotosynthetic isoforms are evolutionarily more closely related to the green algae photosynthetic FNRs than to those of higher plants. Furthermore, the photosynthetic FNR from higher plants is more similar to the cyanobacteria FNR than to the root isoform. Crystal structures of photosynthetic FNRs have been reported from cyanobacteria (*9*) and higher plants [spinach (*10*, *11*), pea (*12*), paprika (*13*), and corn (*14*)], showing that these enzymes are highly similar. Recently, crystal structures of the complex between photosynthetic FNR and Fd have revealed the interactions that are important for complex formation (*14*, *15*). Work on nonphotosynthetic FNRs is much less developed.

Our aim was to highlight the structural and functional differences between the leaf and root isoforms of FNR. The group of Hase (*16*, *17*) has begun to address this problem by studying the specific interactions of corn leaf and corn root FNR with the specific leaf and root isoforms of Fd. Here, we present a thorough characterization of a nonphotosynthetic FNR, reporting on the enzymatic and redox properties, and the 1.7 Å crystal structure of recombinant corn root FNR. These achievements also take on biomedical relevance with the recent discovery of the presence in *Toxoplasma gondii*, a protozoan parasite, of an FNR of the root type (*18*).

[†] This work was supported by grants from Ministero dell'Università e della Ricerca Scientifica e Tecnologica and the CNR Target Project on Biotechnology of Italy, and from the U.S. National Science Foundation (to P.A.K.).

[‡] Atomic coordinates of maize root ferredoxin−$NADP^+$ reductase have been deposited in the RCSB Protein Data Bank as entry 1JB9.

* To whom correspondence should be addressed: Dipartimento di Fisiologia e Biochimica Generali, Università degli studi di Milano, Via Celoria 26, 20133 Milano, Italy. Phone: +39 02 5835 4896. Fax: +39 02 5835 4895. E-mail: gzanetti@mailserver.unimi.it.

[§] Università degli Studi di Milano.

[∥] Oregon State University.

[⊥] Cornell University.

[@] Istituto di Fisiologia Veterinaria e Biochimica.

[1] Abbreviations: FNR, ferredoxin−$NADP^+$ reductase; Fd, ferredoxin; thio-$NADP^+$, thionicotinamide adenine dinucleotide phosphate; DTNB, 5,5′-dithiobis(2-nitrobenzoate); INT, 2-(*p*-iodophenyl)-3-(*p*-nitrophenyl)-5-phenyltetrazolium chloride; e^-eq, electron equivalent.

10.1021/bi011224c CCC: $20.00
Published on Web 11/06/2001

EXPERIMENTAL PROCEDURES

Recombinant, spinach leaf FNR and Fd I were purified from *Escherichia coli* as previously reported (*19*, *20*). Horse heart cytochrome *c* and bovine pancreas trypsin (TPCK-treated) were purchased from Sigma. Restriction endonucleases and T4 DNA ligase were obtained from either Gibco BRL or Boehringer Mannheim. $NADP^+$, NADPH, and thio-$NADP^+$ were all from Sigma. 5′-Deazariboflavin was a generous gift of S. Ghisla (Konstanz, Germany).

Plasmid Construction. Plasmid pETrFNR1, a construct for corn root FNR expression based on vector pET23b, was kindly provided by W. H. Campbell (Houghton, MI) (*6*). Because initial preparations using pETrFNR1 yielded heterogeneous material, pETrFNR2 was constructed from pETrFNR1 by the insertion of a factor Xa recognition site (IleGluGlyArg) in front of the codon of the first amino acid residue of the mature FNR, and by removing a potentially reactive Cys residue by changing the codon for Cys(−6) from TGC to AGC (which encodes Ser). To obtain pETrFNR2, the Sculptor *in vitro* Mutagenesis System (Amersham Pharmacia Biotech) was used in conjunction with the 59mer 5′-GTCGGCGCCAGCAAGGTGCTCAGCATGATCGAGGGTAGGTCCGTCCAGCAGGCGAGCAG-3′. The nucleotides encoding the IleGluGlyArg tetrapeptide and the T → A point mutation are underlined. The insert of pETrFNR2 was checked by sequencing.

Overexpression and Purification of Corn Root FNR. *E. coli* strain BL21(DE3) was transformed with pETrFNR2 and grown at 37 °C in 2×YT medium supplemented with 100 mg/L ampicillin. After induction for 2 h with 0.2 mM isopropyl β-D-thiogalactopyranoside, cells were harvested by centrifugation and stored at −80 °C. The pH of Tris buffers was measured at 25 °C, and unless noted, purification steps were carried out at 4 °C. Frozen cell pellets were suspended in 2 volumes of 100 mM Tris-HCl (pH 7.4), 1 mM EDTA, and 1 mM phenylmethanesulfonyl fluoride and disrupted by sonication. After centrifugation, the crude extract was brought to 40% saturated ammonium sulfate and centrifuged. The supernatant was loaded on a Sepharose 4B (Pharmacia Biotech) column equilibrated with 40% saturated ammonium sulfate in 50 mM Tris-HCl (pH 7.4) and 1 mM EDTA. FNR was eluted with ∼1.5 column volumes of the same solution and then precipitated at 75% saturated ammonium sulfate. The combination of ammonium sulfate fractionation and salt-promoted adsorption chromatography on Sepharose 4B served the double role of removing most contaminants and of concentrating the protein solution. After resuspension and dialysis against 10 mM Tris-HCl (pH 7.4) and 1 mM EDTA, the protein was chromatographed by FPLC (at room temperature) on an SP-Sepharose HP column (Pharmacia Biotech). Elution was performed with a gradient from 0 to 0.5 M NaCl in 10 mM Hepes/NaOH (pH 7.0). To remove the N-terminal extension, the FNR solution was adjusted to 100 mM Tris-HCl (pH 8.0), 2 mM in $CaCl_2$, and incubated with bovine factor Xa (Pierce) at a ratio of 1/3000 (w/w) for ∼12 h at 12 °C. The reaction mixture was brought to 35% saturated ammonium sulfate and loaded on a Phenyl-Sepharose HP column (Pharmacia Biotech). Mature root FNR was then eluted by FPLC (at room temperature) with a gradient from 35 to 0% saturated ammonium sulfate in 50 mM Tris-HCl (pH 8.0). The resulting protein preparation was homogeneous as judged by SDS−PAGE and the A_{276}/A_{459} spectral ratio of 7.6. N-Terminal sequencing confirmed the correct factor Xa processing of the protein.

Spectral Analyses. Absorption spectra were recorded with a Hewlett-Packard 8453 diode-array spectrophotometer. The extinction coefficient of the protein-bound flavin was determined by spectrophotometrically quantitating the FAD released from the apoprotein following sodium dodecyl sulfate treatment, as described in ref *21*. Fluorescence measurements were performed on a Jasco FP-777 spectrofluorometer at 15 °C. For titrations of protein sulfhydryl groups, FNRs at ∼10 μM in 50 mM sodium phosphate (pH 7.0) were reacted with DTNB in the presence and absence of 6 M guanidinium chloride (*22*).

Flavin Photoreduction. Photoreductions using EDTA and light (*23*) were carried out in anaerobic cuvettes at 15 °C, containing 15−20 μM root FNR in 10 mM Hepes, at either pH 7.0 or 8.8, 15 mM EDTA, and 0.4−0.8 μM 5-deazariboflavin, in the absence and in the presence of either $NADP^+$ or NAD^+ (*24*, *25*). Solutions were made anaerobic by successive evacuation and flushing with O_2-free N_2.

Steady-State Kinetics and Interaction with Ligands. Enzyme assays were performed as previously described (*26*). Spectrophotometric titrations of root FNR with $NADP^+$ and thio-$NADP^+$ were performed as described for the leaf enzyme (*25*). Fluorimetric titrations of root FNR with spinach leaf Fd I to obtain the K_d of the protein−protein complex were carried out as described previously (*24*).

Electrophoresis, Limited Proteolysis, and Sequencing. Isoelectrofocusing was carried out on polyacrylamide gels in the pH range of 3.5−10. Conditions of limited proteolysis with trypsin were essentially as previously reported (*27*), with activity time courses followed by assaying both diaphorase and cytochrome *c* reductase activities. Electrophoretic analysis was carried out using 12% SDS−polyacrylamide gels (*28*). After Western blotting on Immobilon P^{SQ} membranes (Millipore) had been carried out, the N-terminal sequences of the polypeptides were obtained using an Applied Biosystems 477/A protein sequencer.

Crystallization. The crystallization behavior of the pure protein [25 mg/mL in 10 mM Hepes (pH 7.0)] was screened in hanging drops (2 μL of sample with 2 μL of reservoir) using the Crystal Screen I and II kits (Hampton Research). At room temperature, crystals were observed within 24 h under many conditions, especially those using polyethylene glycol (PEG) as the precipitant. The best crystals grew under condition 18 [20% PEG 8000, 0.1 M sodium cacodylate (pH 6.5), and 0.2 M magnesium acetate]. Optimization yielded useful crystals over a broad range of conditions between pH 6.0 and 7.0 in cacodylate buffer and between pH 7.6 and 8.5 in 0.1 M Tris buffer, both with and without magnesium acetate. Large (ca. 0.4 mm × 0.4 mm × 0.8 mm) crystals grew within 1 week.

Data Collection. For data collection, crystals were transferred to artificial mother liquor [25% PEG 8000, 0.1 M sodium cacodylate (pH 6.0), and 0.2 M magnesium acetate] and mounted in a capillary. Native data were collected at room temperature on a Rigaku rotating anode X-ray source (50 mA, 100 kV, Cu anode) equipped with an Raxis IV image plate detector set at a distance of 150 mm with a 2θ offset of 13°. Images were collected in 1° oscillations and processed to 1.7 Å resolution using DENZO and SCALEPACK

Table 1: Data Collection and Refinement Statistics

data[a]	
space group	$P3_221$
cell dimensions (Å)	$a = b = 59.67$ Å, $c = 189.10$ Å
resolution (Å)	1.7
no. of measured reflections	246386
no. of unique reflections	43654
completeness (%)	99.1 (97.6)
R_{meas} (%)[b]	6.8 (36.9)
refinement	
resolution limits (Å)	20.0−1.7
R_{cryst} (%)	16.7
R_{free} (%)[c]	22.3
rmsd for bond lengths (Å)	0.013
rmsd for bond angles (deg)	2.1
no. of protein atoms	2505
no. of waters	274

[a] Values for the highest-resolution bin are shown in parentheses. [b] $R_{meas} = \sum_h (n_h/n_h-1)^{1/2} \sum_i |<I_h> - I_{h,i}|/\sum_h \sum_i I_{h,i}$ (*34*). [c] R_{free} was calculated in the penultimate round of refinement against 10% of the total reflections which had not been used in refinement to that point (*33*).

(*29*). Indexing indicated a trigonal space group, and the scaling behaved well using 32 symmetry. Unit cell parameters and data quality statistics are given in Table 1.

Structure Solution and Refinement. Molecular replacement was carried out with the MRX package (*30*). A search model (2013 non-hydrogen atoms) was constructed from spinach FNR (PDB entry 1FNB) using all homologous atoms based on sequence alignment. Using data between 10 and 4 Å resolution, the rotation function for $P3_x21$ (Laue group 3^-m1) gave a solution 5.0σ above the mean (next highest peak at 3.6σ). $P3_x12$ (or Laue group 3^-1m) showed no substantial peaks above the background. The fast translation function gave a solution 7.1σ above the mean (next highest peak at 4.33σ) in space group $P3_121$ and no significant peaks for space group $P3_121$. This molecular replacement solution had an initial *R*-factor of 46.4 for the data between 20 and 4.0 Å resolution.

Crystallographic refinement was carried out using the TNT program suite (*31*), and model building was carried out with O (*32*). Ten percent of the data were set aside for cross-validation (*33*). The data were scaled using the following overall anisotropic scale factors as determined by TNT: $B_{11} = B_{22} = 1.14$, $B_{33} = -2.27$, and $B_{12} = 1.14$. Rigid body refinement at 4.0 Å resolution reduced the *R*-factor to 44.7%, and rounds of positional refinement while slowly extending the resolution to 2.5 Å resolution yielded an *R*-factor of 32.7% ($R_{free} = 45\%$). Initial inspection of $2F_o - F_c$ and $F_o - F_c$ maps clearly showed several loops which were incorrectly placed, density for the N-terminal residues, and a different conformation of the adenosyl portion of the FAD. Subsequent rounds of interactive model building, positional and *B*-value refinement, and resolution extension yielded the current model which has an *R*-factor of 16.7 ($R_{free} = 22.3$) at 1.7 Å resolution. During model building, water molecules were added to $F_o - F_c$ electron density peaks of $>3.0\sigma$ if at least one H-bond could be made. Waters that exhibited little $2F_o - F_c$ density were subsequently removed from the structure. Residues 1−5 and 242−245 have no density and have not been modeled. Statistics of the final model are given in Table 1.

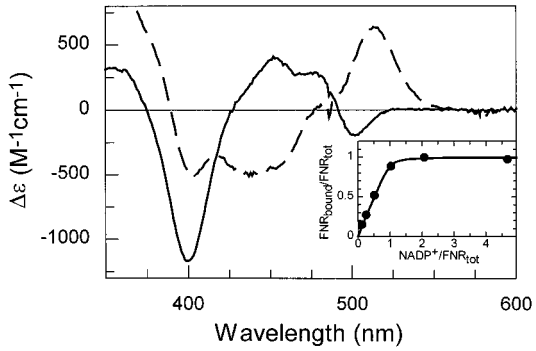

FIGURE 1: Difference absorption spectra elicited by binding of $NADP^+$ and thio-$NADP^+$ to root FNR. Difference spectra obtained by subtracting the spectrum of the unliganded FNR from that of its saturated complexes with $NADP^+$ and thio-$NADP^+$: (—) $NADP^+$ complex and (− − −) thio-$NADP^+$ complex. The inset shows the titration of root FNR with $NADP^+$. The curve represents the theoretical equation for a 1/1 binding stoichiometry with a K_d of 0.3 μM.

RESULTS

Molecular and Catalytic Characterization. The newly designed pETrFNR2 expression system and preparation yielded ~8 mg of pure native recombinant corn root FNR per liter of culture. The protein ran as a single band with a pI of 6.9 on isoelectric focusing. The root FNR displayed a typical flavoprotein spectrum with maxima at 387 and 459 nm ($\epsilon_{459} = 9.3$ mM^{-1} cm^{-1}), and the flavin fluorescence was nearly fully quenched.

As expected, corn root FNR was very active in both the diaphorase (Table 2) and Fd-dependent cytochrome *c* reductase assays (Table 3) that are commonly used to characterize FNRs from photosynthetic tissues. In the diaphorase reactions, root FNR exhibited an unexpectedly low K_m for NADPH, suggesting tight binding of this substrate. Corn root FNR also strongly differentiates between NADPH and NADH with the k_{cat}/K_m^{NADH} for the NADH−ferricyanide reduction being 130000-fold lower than that with NADPH [k_{cat} and K_m^{NADH} are 1 e^-eq/s and 1.3 mM, respectively]. In the cytochrome *c* reductase assay, we used the readily available spinach Fd I as the intermediate electron acceptor. Because plant Fds are well conserved (*35*, *36*), we expect the main difference between the leaf (Fd I) and root (Fd III) isozymes to be the redox potential: $E'_0 = -321$ mV for Fd III (*16*) versus $E'_0 = -401$ mV for Fd I (*37*). To assess the effect of the redox potential, two mutants of Fd I (E92A and E92K) of more positive potential [−323 and −308 mV, respectively (*37*, *38*)] were also tested (Table 3). The k_{cat} values obtained with these mutants were more than double that measured with wild-type Fd I, while K_m and K_d values were similar for all the Fd I forms.

Interactions with $NADP^+$ and Thio-$NADP^+$. The steady-state kinetic studies suggested the root enzyme has a high affinity for NADPH, and this was confirmed by spectrophotometric titrations with $NADP^+$. The affinity for $NADP^+$ was high enough to make an accurate determination of the dissociation constant difficult. A K_d of ≤ 0.3 μM was estimated (Figure 1, inset). For FNRs, additional information is provided by the $\Delta\epsilon_{510}$ value from the difference spectrum, which is proportional to the fraction of molecules for which the nicotinamide ring of the pyridine nucleotide is bound near the flavin, as opposed to being disordered (*12*, *25*, *39*).

Table 2: Kinetic Parameters of the Corn Root FNR for the Diaphorase Reactions with Different Electron Acceptors

electron acceptor	k_{cat} (e^-eq/s)	K_m^{NADPH} (μM)	k_{cat}/K_m^{NADPH} (e^-eq s^{-1} μM^{-1})	$K_m^{acceptor}$ (μM)	$k_{cat}/K_m^{acceptor}$ (e^-eq s^{-1} μM^{-1})
$K_3Fe(CN)_6$	520 ± 10	12 ± 1	43 ± 4	100 ± 10	5.2 ± 0.6
INT	140 ± 20	10 ± 4	14 ± 6	185 ± 25	0.75 ± 0.1

Table 3: Kinetic Parameters of the Corn Root FNR for the Fd-Dependent NADPH−Cytochrome *c* Reductase Reaction and Dissociation Constants of the Oxidized Fd I−FNR Complexes

Fd I form	$E°$ (mV)	k_{cat} (e^-eq/s)	K_m^{Fd} (μM)	k_{cat}/K_m (e^-eq s^{-1} μM^{-1})	K_d[a] (μM)
wild type	−401	115 ± 3	2.5 ± 0.2	46 ± 4	0.15 ± 0.01
E92A	−323	265 ± 5	1.9 ± 0.1	140 ± 8	0.17 ± 0.03
E92K	−308	276 ± 7	2.3 ± 0.1	120 ± 6	0.13 ± 0.02

[a] Determined by fluorimetric titration.

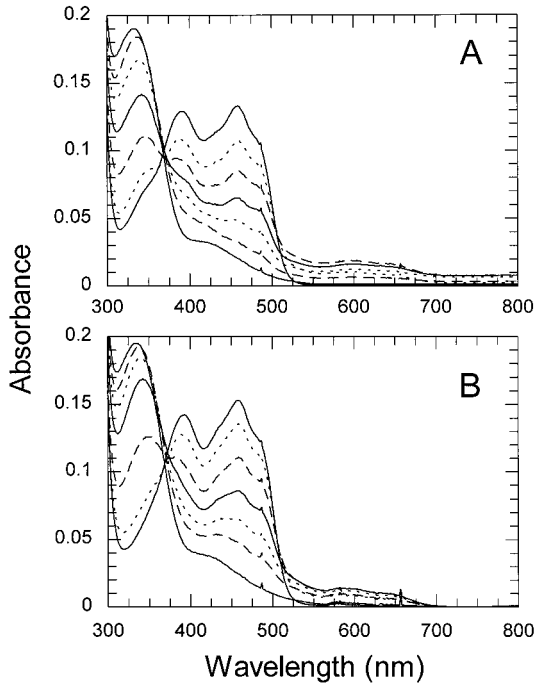

FIGURE 2: Photoreduction of root FNR. Absorbance spectra of anaerobic FNR solutions recorded at successive stages of reduction. Spectra were not corrected for the spectral contribution of 5-deazariboflavin. (A) Reduction performed in the presence of an equimolar amount of $NADP^+$, with the weak absorbance bands near 600 and 750 nm being due to the flavin semiquinone (FADH*) and charge-transfer complexes with NADP(H), respectively (*24*, *25*). (B) Reduction performed in the presence of an equimolar amount of NAD^+.

For corn root FNR, the difference spectra (Figure 1) show that $NADP^+$ induces a small negative peak at 510 nm ($\Delta\epsilon_{500}$ = −0.19 mM^{-1} cm^{-1}), whereas thio-$NADP^+$ binding produces the expected positive peak ($\Delta\epsilon_{514}$ = 0.64 mM^{-1} cm^{-1}).

Photoreduction. Stepwise anaerobic photoreductions of the FAD prosthetic group of root FNR were performed for the free enzyme (data not shown), and in the presence of $NADP^+$ (Figure 2A). As for other FNRs, the root isoform stabilized the neutral blue semiquinone form of FAD (FADH*). The maximal amount of FADH* formed was 19% of the total FAD, both in the presence and in the absence of an equimolar amount of $NADP^+$. Photoreductions were also performed in the presence of NAD^+, as a redox indicator (Figure 2B). Although NAD(H) is a poor ligand of FNR, it exchanges

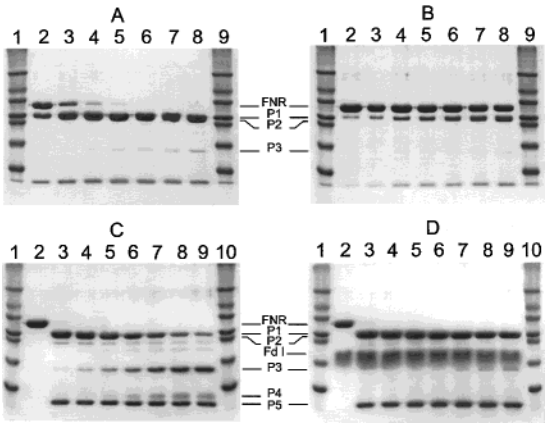

FIGURE 3: Limited proteolysis of root FNR. Time course of fragmentation of root FNR by trypsin under various conditions as analyzed by SDS−PAGE. Treatment with 0.5% (w/w) trypsin in the absence (A) or presence (B) of 1 mM $NADP^+$. Lanes 2−8 are after incubation for 1, 5, 10, 15, 20, 30, and 40 min, respectively. Treatment with 10% (w/w) trypsin in the absence (C) or presence (D) of a 6-fold excess Fd I. Lanes 2−9 are after incubation for 0, 1, 5, 10, 20, 40, 80, and 120 min, respectively. Molecular mass markers in the edge lanes are at 66, 45, 36, 29, 24, 20, and 14.2 kDa. Peptides are identified as in Table 4.

electrons with the FNR-bound FAD rapidly enough for the redox equilibrium to be easily reached after each light irradiation period. The weakness of FNR−NAD(H) interactions greatly facilitates spectral analysis since no charge-transfer species are observed. In separate experiments, under the same conditions, spinach leaf and corn root enzymes were photoreduced in the presence of NAD^+ and their spectra analyzed. Nernst plots for the two-electron reduction of the FAD bound to the root FNR at pH 7 yielded an E'_m of −337 mV, whereas the redox potential of the leaf isoform was found to be 19 mV more negative, a value close to that determined by potentiometry (*40*). Independent titrations at pH 8.8 yielded a similar 26 mV difference in the same direction.

Limited Proteolysis. To characterize the flexibility and involvement in substrate binding of surface regions of root FNR, limited proteolysis experiments have been carried out (Figure 3). Proteolysis with 0.5 and 10% (w/w) trypsin (panels A and C, respectively) revealed that root FNR was first cleaved into fragments of ∼29 and ∼9 kDa (cleavage at site 1), and much more slowly, the 29 kDa polypeptide was shortened to a 28 kDa fragment (cleavage at site 2), and cleaved into fragments of ∼18 and ∼10 kDa (cleavage at site 3). The cleavages at sites 2 and 3 appear to be coupled to one another as there is little buildup of the 28 kDa fragment. Amino-terminal sequencing of all major bands observed via SDS−PAGE (Table 4) identified site 1 as Lys247, site 2 as Arg7, and site 3 as Lys82. Panels B and D reveal that $NADP^+$ binding slowed the cleavage at Lys247, and Fd I binding slowed the cleavage at Lys82. Limited proteolysis of FNR with trypsin resulted in the loss of most of its diaphorase and cytochrome *c* reductase activities.

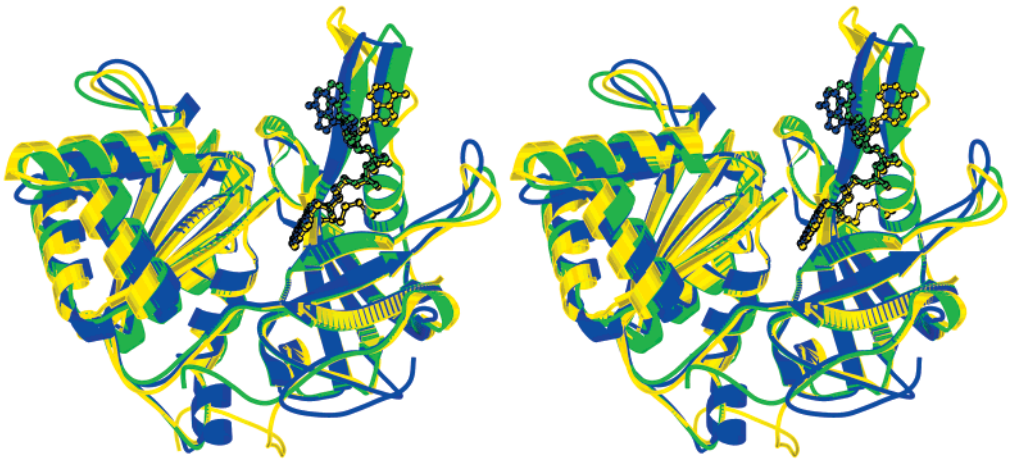

FIGURE 4: Corn root FNR structure compared with photosynthetic FNRs. A stereoview shows that the corn root FNR structure (yellow) is highly similar to those of spinach leaf FNR (green) and *Anabaena* FNR (blue). FAD is shown as a ball-and-stick model. The structurally common region of the proteins begins with Glu22 (Gly26 in spinach FNR and Asp9 in *Anabaena* FNR) and extends through the C-terminus of each protein. Three unique features of corn root FNR are the conformation of the amino-terminal extension, the conformation of the FAD adenosyl moiety, and the presence of a disulfide bond (shown as a ball-and-stick model) in the FAD binding domain.

Table 4: Identification of Proteolytic Products Released by Trypsin

peptide	M_r[a]	N-terminal sequence	fragment (M_r)[b]
P1	29	SVQQASR	Ser1−Lys247 (27.2)
P2	28	SKVSVAPLHLESAK	Ser8−Lys247 (26.2)
P3	18	KPGAPQNVRLYSIA	Lys83−Lys247 (18.5)
P4	10	SKVSVAPLHL	Ser8−Lys82 (8.0)
P5	9	MYVQDK	Met248−Tyr316 (8.1)

[a] The M_r (multiplied by 10^{-3}) based on the mobility in SDS gel electrophoresis. [b] The C-terminus of each fragment is inferred, and the approximate computed M_r (multiplied by 10^{-3}) is given in parentheses.

Interestingly, the proteolyzed enzyme maintained an activity of ~1200 units/FAD in both ferricyanide and cytochrome *c* reductase reactions, to be compared with the native enzyme values of 25 000 and 6000 units/FAD, respectively. Under all the conditions that were tested, inactivation occurred as a single-exponential decay process, with both diaphorase and cytocrome *c* reductase activities being lost at the same rate. At 0.5% trypsin, the half-time was ~3 min, suggesting by comparison with SDS−PAGE data (Figure 3A) that activity loss resulted from cleavage at site 1 (Lys247). Indeed, $NADP^+$ binding afforded nearly complete protection against inactivation (see Figure 3B), whereas Fd I had no effect. At 10% trypsin, FNR inactivation was too fast to allow determination of the half-life. Within 1 min, the fast phase was completed and no further inactivation occurred. Thus, cleavage at site 3, which occurs at a considerably slower rate than digestion at site 1 (Figure 3C), did not result in an additional decrease in diaphorase or cytochrome *c* reductase activity.

Crystal Structure of Corn Root FNR. The structure at 1.7 Å resolution reveals a two-domain protein that is globally similar to the FNRs from photosynthetic tissues (Figure 4). The FAD-binding domain is a six-stranded β-barrel spanning residues 8−155, and the NADP-binding domain is a five-stranded parallel α/β-sandwich spanning residues 165−316. While the majority of the structure is well-ordered, residues 1−8, 81−86, and 239−247 are very disordered ($B > 70$ Å^2 or not modeled), and details of the model in these regions are not reliable. Since the structural features of FNRs from photosynthetic tissues have been well described, we will focus our comments on three features of the root FNR structure that are distinct.

As seen in Figure 4, the common structural core of all FNRs begins with Glu22. Corn root FNR has 13 well-ordered residues preceding this residue that extend away from the exposed edge of the flavin making contacts with residues that are well conserved among root FNR sequences, but distinct from other FNR sequences. A second major difference is the conformation of the adenosyl portion of the FAD molecule bound to FNR (Figure 4). This change in conformation appears to be associated with a four-residue insertion altering the conformation of the loop that interacts with the adenosyl moiety. The difference in the FAD conformation involves an ~120° rotation about the C5′−C4′ bond and an ~20° rotation of the O5′−C5′ bond. A third intriguing feature is the formation of a disulfide bridge between Cys54 and Cys139 (Figure 5). The disulfide is very well ordered and is mostly buried, with a slight accessibility of the Cys54 side chain.

To assess if the disulfide is present in the enzyme in solution, a DTNB titration of free thiols was performed on root FNR. Spinach leaf FNR, which does not contain disulfides (*10*, *41*), was used as a control. In both corn root and spinach leaf FNR forms, cysteinyl side chains were not accessible to titrant under native conditions. Titrations performed in the presence of 6 M guanidinium hydrochloride indicated that, while both FNR forms contain five cysteinyl residues, a different number of them are present as free thiols in the two proteins: all five in the leaf form (4.6 mol of −SH/mol of FAD) and three in the root enzyme (2.8 mol of −SH/mol of FAD). This confirmed that two cysteines form a disulfide bridge in root FNR also in solution. Attempts to reduce the disulfide by overnight incubation of the enzyme with 1 mM β-mercaptoethanol or 50 mM DTT were unsuccessful as judged by DTNB titration following gel filtration to eliminate excess reagent.

DISCUSSION

This biochemical characterization of corn root FNR provides a basis for assessing what structural and enzymatic differences are associated with the differing physiological

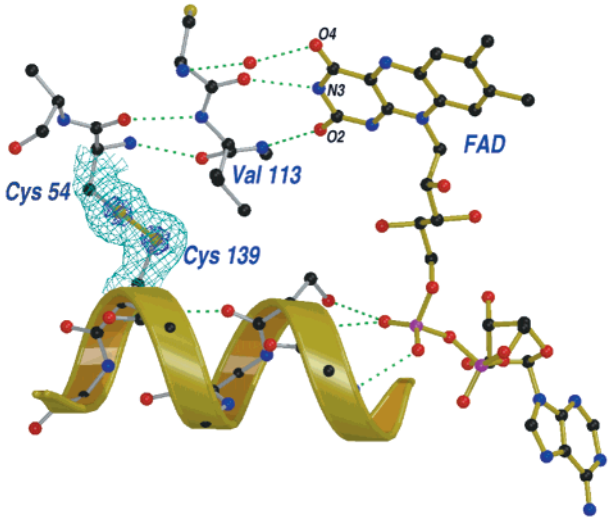

FIGURE 5: Disulfide bond in corn root FNR. The image shows the refined model and the $2F_o - F_c$ 1.7 Å electron density map (contour levels at $2.0\rho_{rms}$ and $7.0\rho_{rms}$). As can be seen, the disulfide is only one layer of protein atoms away from both the flavin ring and the FAD pyrophosphate. Gly132, Cys134, and Ser135 are conserved in all FNR sequences. Hydrogen bonds (<3.2 Å) are shown as dashed lines.

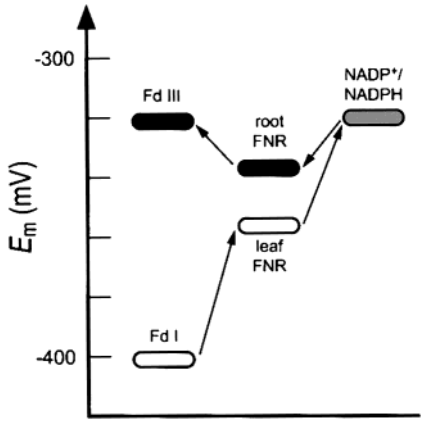

FIGURE 6: Physiological electron flow in the leaf and root Fd/FNR systems. The redox potentials of the couples involved are reported on the vertical axis. Leaf proteins are represented by empty boxes and root proteins by filled ones. Arrows indicate the physiological flow of electrons in the protein systems. The potentials that are shown are −321 mV for root Fd (*16*), −401 mV for leaf Fd (*37*), −337 mV for root FNR (this work), −356 mV for leaf FNR (this work), and −320 mV for the NADPH/$NADP^+$ couple.

roles of FNRs from photosynthetic and nonphotosynthetic tissues. Because FNRs from photosynthetic tissues as diverse as spinach and cyanobacteria have very similar characteristics (*8*, *35*, *42*), these can be compared as a group with corn root FNR. The spectral, catalytic, and structural features of corn root FNR are rather similar to those of FNRs from photosynthetic tissues. This is consistent with the similar functions they carry out, however. In the discussion here, we will focus on those properties that differ, and attempt to assess why they differ and how that relates to the functional differences of the enzymes.

Apparently, the redox potential of FNRs has been tuned for the physiological direction of electron transport (Figure 6). For Fds, the redox potential is dramatically adjusted for function, with root Fd (Fd III) having a potential nearly 100 mV higher than that of leaf Fd I, so that it can be effectively reduced by the NADPH/$NADP^+$ couple. While the effect for FNRs is less impressive, the near 20 mV difference between the isoform redox potentials puts the three redox couples of the root system almost at the same level. Furthermore, it should be recalled that the redox potential (E_m) of the spinach leaf FNR became more positive (∼20 mV) by complexation with Fd (*43*, *44*), the major change being in the E_m of Fd, which became more negative: −75 (*43*) or −25 mV (*44*). If the same change occurs by complex formation of the root proteins, it will bring the E_m of root FNR isopotential with that of the NADPH/$NADP^+$ couple, thus favoring the electron flow in the physiological direction. Nevertheless, it is envisaged that the E_m of the root Fd in the complex should not become more negative but rather more positive to allow for more efficient electron transfer from FNR to Fd.

In terms of the specificity of FNRs for their counterpart Fds (Fd I−leaf FNR and Fd III−root FNR), Onda et al. (*17*) showed that leaf FNR does not discriminate between Fd I and Fd III, but that root FNR discriminates against Fd I by a factor of 10 in affinity. However, we found that our K_d and K_m values for the root FNR−Fd I complex are much lower and are comparable to those of the leaf FNR−Fd I complex. While the reason of these discrepancies is not clear, it should be noted that the conditions used in our assay are quite different with regard to ionic strength, concentrations of cytochrome *c*, and fixed substrate. On the other hand, one new insight revealed by our experiments with mutant Fds is that the k_{cat} values for cytochrome *c* reduction depended strongly on the Fd redox potential (Table 3 and refs *37* and *38*). This trend was not seen by Onda et al. (*17*). Further experiments to clarify these discrepancies are being pursued.

A second notable difference in the two isoforms involves the binding of NADP(H). The root FNR shows a much higher affinity for $NADP^+$ ($K_d \leq 0.3$ μM), but as judged from the difference spectrum (Figure 1), occupancy of the active site by the nicotinamide ring is lower. Indeed, the $NADP^+$−root FNR difference spectrum closely resembles that of the leaf enzyme with ATP ribose, a $NADP^+$ analogue lacking the nicotinamide ring (*39*). In the framework of the bipartite binding model for the NADP interaction with leaf FNR (*12*), root FNR has a 2′-phospho-AMP binding subsite with higher affinity and a NMN binding subsite with lower affinity in comparison to those of the leaf enzyme. We suspect a key difference in structure that causes this increase in affinity for the 2′-phospho-AMP portion of NADP is that root FNRs have increased positive charge in this region as compared to the leaf FNRs. In particular, in positions 238, 240, and 243 (spinach leaf FNR numbering), leaf FNRs have Thr/Val, Glu/Asp/Ala, and Glu, whereas root FNRs have Lys, Lys/Arg/Asn, and Gly, respectively. Another possible contributor is that Lys116 of leaf FNRs (spinach numbering), whose side chain contacts the pyrophosphate of NADP (*12*), is replaced with an Arg in all root FNRs, and this may provide a stronger interaction. With regard to the possible functional aspect of this tighter binding of the NADPH/$NADP^+$ couple by the root isoform, Jin et al. (*45*) have reported a strong inhibition by $NADP^+$ of nitrite reduction in an in vitro reconstituted electron transport system from the green alga *Chlamydomonas reinhardtii* (NADPH, FNR, Fd, nitrite reductase, and nitrite). They showed that FNR was the target of the inhibition.

A third biochemical distinction is that the proteolytic sensitivity patterns of root FNR (cleavage at residues 7, 82, and 247) differ from those of spinach leaf FNR, which was susceptible to proteolysis at the N-terminus up to residue 35, and in the segment of residues 235−250 (*27*). In each case, however, the limited proteolysis sites correspond to poorly ordered regions of the crystal structure. In particular, the 240's loop is disordered in both structures, the N-terminus is folded better in the root FNR structure, and the 80's loop is less ordered in the root FNR structure as part of the different binding of the adenosine portion of FAD (Figure 4). For corn root FNR, limited proteolysis resulted in a substantial but not complete impairment of catalytic function, whereas it fully inactivated spinach leaf FNR. The effect on activity of the former is entirely due to cleavage within the 240's loop (site 1), cleavages in the N-terminal domain (sites 2 and 3) having no additional effect on residual enzyme activity. All these observations strongly suggest that, once cleaved, peptides P4, P3, and P5 do not dissociate, providing a nicked, partially active enzyme form. In the case of spinach leaf FNR, the 240's loop was disrupted by at least two cleavages (*27*). For corn root FNR, protection of the 240's loop (site 1) by $NADP^+$ and protection of the 80's loop by Fd I are consistent with their expected roles in substrate binding based on biochemical (*19*, *46*, *47*) and structural studies (*12*, *14*, *15*) of the photosynthetic FNRs.

Each of the three novel structural features seen in the corn root FNR structure (Figure 4) involves residues that are well-conserved among root enzymes, but distinct from other FNRs, leading us to propose that these properties are common to all root FNRs. The structural change at the N-terminus affects the surface of FNR that interacts with Fd, and so may be important for the distinct recognition of root type Fds (see also below). The distinct placement of the adenosyl part of FAD is distant from the active site, and we suggest it does not have specific functional implications. The disulfide bond is a most intriguing feature, because disulfide bonds are rather uncommon in intracellular proteins, and because it is known that the regulation of a number of plastid enzymes involves the reduction or formation of disulfide bonds (*48*−*50*). This leads us to speculate as to whether this disulfide bridge may play a functional (regulatory) role. Although the disulfide is not directly adjacent to the active site, it is relatively close (∼8 Å), and is structurally connected to the FAD binding in two ways (Figure 5). First, Cys54 makes β-sheet interaction with residues 112−114 whose backbone atoms make H-bonds with the edge of the flavin. Second, Cys139 is in the highly conserved first turn of an α-helix that binds the FAD pyrophosphate. Either of these connections could allow the reduction of this disulfide to have significant effects on enzyme activity. Interestingly, while Cys54 and Cys139 are conserved in all plant root and algal FNRs, Cys54 is not conserved in the nonphotosynthetic FNR from the apicoplast of *T. gondii* (*18*).

In conclusion, characterization of the biochemical and structural properties of corn root FNR led us to conclude that its redox potential differs from that of leaf FNR in a small but significant way that enhances the thermodynamics of catalysis (Figure 6). Two additional differences we have discovered involve the tighter binding of NADP(H) by the root enzyme and the presence of a disulfide bond in the root enzyme. Whereas the functional importance of these latter differences is unknown, they raise questions about the levels of the NADPH/$NADP^+$ couple in the root plastid, and the possibility of redox regulation of nitrogen fixation enzymes.

REFERENCES

1. Morigasaki, S., Takata, K., Sanada, Y., Wada, K., Yee, B. C., Shin, S., and Buchanan, B. B. (1990) *Arch. Biochem. Biophys. 283*, 75−80.
2. Morigasaki, S., Takata, K., Suzuki, T., and Wada, K. (1990) *Plant Physiol. 93*, 896−901.
3. Hirasawa, M., Chang, K.-T., and Knaff, D. B. (1990) *Arch. Biochem. Biophys. 276*, 251−258.
4. Bowsher, C. G., Hucklesby, D. P., and Emes, M. J. (1993) *Plant J. 3*, 463−467.
5. Aoki, H., and Ida, S. (1994) *Biochim. Biophys. Acta 1183*, 553−556.
6. Ritchie, S. W., Redinbaugh, M. G., Shiraishi, N., Vrba, J. M., and Campbell, W. H. (1994) *Plant Mol. Biol. 26*, 679−690.
7. Oelmüller, R., Bolle, C., Tyagi, A. K., Niekrawietz, N., Breit, S., and Herrmann, R. G. (1993) *Mol. Gen. Genet. 237*, 261−272.
8. Arakaki, A. K., Ceccarelli, E. A., and Carrillo, N. (1997) *FASEB J. 11*, 133−140.
9. Serre, L., Vellieux, F. M. D., Medina, M., Gómez-Moreno, C., Fontecilla-Camps, J. C., and Frey, M. (1996) *J. Mol. Biol. 263*, 20−39.
10. Karplus, P. A., Daniels, M. J., and Herriott, J. R. (1991) *Science 251*, 60−66.
11. Bruns, C. M., and Karplus, P. A. (1995) *J. Mol. Biol. 247*, 125−145.
12. Deng, Z., Aliverti, A., Zanetti, G., Arakaki, A. K., Ottado, J., Orellano, E. G., Calcaterra, N. B., Ceccarelli, E. A., Carrillo, N., and Karplus, P. A. (1999) *Nat. Struct. Biol. 6*, 847−853.
13. Dorowski, A., Hofmann, A., Steegborn, C., Boicu, M., and Huber, R. (2001) *J. Biol. Chem. 276*, 9253−9263.
14. Kurisu, G., Kusunoki, M., Katoh, E., Yamazaki, T., Teshima, K., Onda, Y., Kimata-Ariga, Y., and Hase, T. (2001) *Nat. Struct. Biol. 8*, 117−121.
15. Morales, R., Charon, M. H., Kachalova, G., Serre, L., Medina, M., Gómez-Moreno, C., and Frey, M. (2000) *EMBO Rep. 1*, 271−276.
16. Akashi, T., Matsumura, T., Ideguchi, T., Iwakiri, K., Kawakatsu, T., Taniguchi, I., and Hase, T. (1999) *J. Biol. Chem. 274*, 29399−29405.
17. Onda, Y., Matsumura, T., Kimata-Ariga, Y., Sakakibara, H., Sugiyama, T., and Hase, T. (2000) *Plant Physiol. 123*, 1037−1045.
18. Vollmer, M., Thomsen, N., Wiek, S., and Seeber, F. (2001) *J. Biol. Chem. 276*, 5483−5490.
19. Aliverti, A., Corrado, M. E., and Zanetti, G. (1994) *FEBS Lett. 343*, 247−250.
20. Piubelli, L., Aliverti, A., Bellintani, F., and Zanetti, G. (1995) *Protein Expression Purif. 6*, 298−304.
21. Aliverti, A., Curti, B., and Vanoni, M. A. (1999) in *Methods in Molecular Biology, Volume 131, Flavoprotein Protocols* (Chapman, S. K., and Reid, G. A., Eds.) pp 9−23, Humana Press, Totowa, NJ.
22. Glazer, A. N., DeLange, R. J., and Sigman, D. S. (1975) *Chemical Modification of Proteins. Selected Methods and Analytical Procedures*, pp 113−114, North-Holland Publishing, Amsterdam.
23. Massey, V., and Hemmerich, P. (1977) *J. Biol. Chem. 252*, 5612−5614.
24. Aliverti, A., Bruns, C. M., Pandini, V. E., Karplus, P. A., Vanoni, M. A., Curti, B., and Zanetti, G. (1995) *Biochemistry 34*, 8371−8379.
25. Aliverti, A., Deng, Z., Ravasi, D., Piubelli, L., Karplus, P. A., and Zanetti, G. (1998) *J. Biol. Chem. 273*, 34008−34015.
26. Aliverti, A., Piubelli, L., Zanetti, G., Lübberstedt, T., Herrmann, R. G., and Curti, B. (1993) *Biochemistry 32*, 6374−6380.
27. Gadda, G., Aliverti, A., Ronchi, S., and Zanetti, G. (1990) *J. Biol. Chem. 265*, 11955−11959.

28. O'Farrell, P. H. (1975) *J. Biol. Chem. 250*, 4007−4021.
29. Otwinowski, Z., and Minor, W. (1997) *Methods Enzymol. 276*, 307−326.
30. Zhang, X.-J., and Matthews, W. B. (1994) *Acta Crystallogr. D50*, 675−686.
31. Tronrud, D. E. (1997) *Methods Enzymol. 277*, 306−319.
32. Jones, T. A., Zou, J.-Y., Cowan, S. W., and Kjeldgaard, M. (1991) *Acta Crystallogr. A47*, 110−119.
33. Brunger, A. T. (1997) *Methods Enzymol. 276*, 366−396.
34. Diederichs, K., and Karplus, P. A. (1997) *Nat. Struct. Biol. 4*, 269−275.
35. Knaff, D. B. (1996) in *Oxygenic Photosynthesis: The Light Reactions* (Ort, D. R., and Yocum, C. F., Eds.) Vol. 4, pp 333−361, Kluwer, Dordrecht, The Netherlands.
36. Zanetti, G., Binda, C., and Aliverti, A. (2001) in *Handbook of Metalloproteins* (Messerschmidt, A., Huber, R., Poulos, T., and Wieghardt, K., Eds.) Wiley, Chichester, U.K.
37. Aliverti, A., Hagen, G., and Zanetti, G. (1995) *FEBS Lett. 368*, 220−224.
38. Piubelli, L., Aliverti, A., Bellintani, F., and Zanetti, G. (1996) *Eur. J. Biochem. 236*, 465−469.
39. Piubelli, L., Aliverti, A., Arakaki, A. K., Carrillo, N., Ceccarelli, E. A., Karplus, P. A., and Zanetti, G. (2000) *J. Biol. Chem. 275*, 10472−10476.
40. Corrado, M. E., Aliverti, A., Zanetti, G., and Mayhew, S. G. (1996) *Eur. J. Biochem. 239*, 662−667.
41. Yao, Y., Wada, K., Takahashi, Y., Katoh, S., and Matsubara, H. (1985) *J. Biochem. 98*, 1079−1082.
42. Zanetti, G., and Aliverti, A. (1991) in *Chemistry and Biochemistry of Flavoenzymes* (Müller, F., Ed.) Vol. 2, pp 305−315, CRC Press, Boca Raton, FL.
43. Batie, C. J., and Kamin, H. (1981) *J. Biol. Chem. 256*, 7756−7763.
44. Smith, J. M., Smith, W. H., and Knaff, D. B. (1981) *Biochim. Biophys. Acta 635*, 405−411.
45. Jin, T., Huppe, H. C., and Turpin, D. H. (1998) *Plant Physiol. 117*, 303−309.
46. Zanetti, G., Morelli, D., Ronchi, S., Negri, A., Aliverti, A., and Curti, B. (1988) *Biochemistry 27*, 3753−3759.
47. Aliverti, A., Lübberstedt, T., Zanetti, G., Herrmann, R. G., and Curti, B. (1991) *J. Biol. Chem. 266*, 17760−17763.
48. Schürmann, P., and Jacquot, J.-P. (2000) *Annu. Rev. Plant Physiol. Plant Mol. Biol. 51*, 371−400.
49. Neuhaus, H. E., and Emes, M. J. (2000) *Annu. Rev. Plant Physiol. Plant Mol. Biol. 51*, 111−140.
50. Jacquot, J.-P., Lancelin, J.-M., and Meyer Y. (1997) *New Phytol. 136*, 543−570.

BI011224C